DOI: http://doi.org/10.25728/cs.2022.2.4

THE HANDLING-COMFORT TRADE-OFF IN A QUARTER-CAR SYSTEM: AUTOMATIC ADAPTIVE MANAGEMENT VIA ACTIVE DISTURBANCE REJECTION CONTROL

M. Alhelou[1], Y. Wassouf[2], V.V. Serebrenny[3], A.I. Gavrilov[4], and E.S. Lobusov[5]

Bauman Moscow State Technical University, Moscow, Russia

[1]✉ alkhelum@student.bmstu.ru [2]✉ thelegend990@gmail.com [3]✉ vsereb@bmstu.ru
[4]✉ alexgavrilov@mail.ru [5]✉ evgeny.lobusov@yandex.ru

Abstract. The effectiveness of a vehicle suspension is often assessed by maximum passenger comfort given continuous contact with the road (road holding). This paper investigates managing the comfort-handling trade-off in a quarter-car suspension system via active disturbance rejection control (ADRC). An adaptive control law is built to manage this trade-off automatically depending on the ADRC parameters. The idea is to use the ADRC-estimated disturbance signal to adjust the system's domain of interest. The effectiveness of the proposed approach is validated: the adaptive control law is tested for a nonlinear hydraulic suspension system. Moreover, the effects of road disturbances amplitudes and road quality on the system performance are studied. Simulation results show the smoothness and simplicity of the adaptive algorithm for managing the comfort-handling trade-off.

Keywords: active disturbance rejection control (ADRC), quarter-car model (QCM), tracking differentiator (TD), nonlinear state error feedback (NLSEF), extended state observer (ESO), disturbance rejection scheme (DRS), proportional-integral-differential (PID) controller, proportional-differential (PD) controller, road handling, ride comfort, road holding, gradient MIT rule (adaptive control method).

INTRODUCTION

A vehicle suspension (suspension system) is a set of parts, components, and mechanisms linking the vehicle body with the road [1]. The suspension performs the following functions:

– It physically connects the wheels or axle assembly to the vehicle's supporting frame.

– It passes to the supporting frame the forces and moments resulting from the interaction of the wheels with the road.

– It ensures the required movement of the wheels relative to the frame and the required smoothness of motion.

When a vehicle moves along a periodic profile with unsprung mass resonances, significant vibrations can occur in its vertical responses to road disturbances. The works [2–6] were devoted to vibrations in vehicle suspension systems. Until recently, when increasing the smoothness of a vehicle, engineers were limited to controlled suspensions to stabilize the position of the vehicle body, mainly its longitudinal (pitch) angle. This contributes to the safe operation of the vehicle by affecting its stability. However, the vehicle's safety in terms of motion instability depends not only on the intensity of vertical, longitudinal-angular, and transverse-angular vibrations of the suspension mass. In the sense of road safety, intense vibrations of the unsprung mass can also be extremely dangerous and therefore undesirable. When moving on periodic bumps under a lateral external force, the vehicle may become unstable due to the weakening of vertical road reactions to the wheels.

A controlled suspension is a type of suspension that adjusts in motion the vertical movement of the wheels relative to the vehicle chassis or body using a special control system. Controlled suspensions can be divided into two classes: active and semi-active. Engineers developed various modifications of automated suspension systems, including active and semi-active spring-based systems [7–10]. Semi-active suspensions change somehow the damping coefficient of the shock absorber to influence the magnitude of the forces generated by it. The corresponding changes in the damping coefficient of the shock absorber depending on the current driving mode of the vehicle are calculated by the control unit based on the information received from the sensor system. Active suspensions include an actuator to control the distance between the wheel center and the chassis.

The smooth ride of a vehicle makes the trip comfortable and minimizes damage to cargo. Moreover, it can minimize the driver's effort during long trips in uncomfortable vehicles [11, 12]. Road handling characterizes how vehicle's wheels respond to the driver's commands and how it moves on the highway or road. This is usually judged by observing the behavior of the vehicle, especially during cornering, acceleration, and braking, as well as by the stability of the vehicle during steady-state motion [13].

Suspension design is often a trade-off between ride comfort and road handling: vehicles with stiff suspension have better regulation of body movements and faster response. Similarly, a low center of gravity is more convenient for road handling, but low ground clearance limits suspension deflection, requiring stiffer springs [8, 14].

In [15], the comfort-handling trade-off was investigated for off-road vehicles on three examples. The authors proposed design criteria for a semi-active suspension system that could significantly reduce or even eliminate the contradiction between ride comfort and road handling. Such a system switches between a stiff spring with high damping mode (for road handling) and a soft spring with low damping mode (for ride comfort). In [10], an automotive active pneumatic system with the main handling and comfort characteristics was presented. The active pneumatic suspension system uses a set of equations for the quarter-car model, a pneumatic valve, and a pneumatic spring. A nonlinear control algorithm based on the *backstepping* principle was adopted. In [16], controllers for improving road holding and passengers' comfort were constructed and analyzed. According to the results, both controllers demonstrate good performance, but the controller proposed below has better performance and reliability.

The contributions of this paper are as follows.

– We propose a new simple and easily adjustable adaptive control system based on *active disturbance rejection control* (ADRC). This control system changes the control domain depending on road disturbances.

– The control strategy is scaled with a single planning parameter and automatically manages the handling-comfort trade-off in the quarter-car model.

– We apply this control algorithm to a hydraulically actuated suspension system.

– We illustrate the effectiveness of the proposed approach using some simulation examples.

1. THE QUARTER-CAR MODEL

The linear active suspension system is shown in Fig. 1. The system dynamics are described by the equations

$$m_s\ddot{z}_s = -K_s(z_s - z_{us}) - C_s(\dot{z}_s - \dot{z}_{us}) + u,$$
$$m_{us}\ddot{z}_{us} = K_s(z_s - z_{us}) + C_s(\dot{z}_s - \dot{z}_{us}) -$$
$$K_{us}(z_{us} - z_r) - C_{us}(\dot{z}_{us} - \dot{z}_r) - u,$$

with the following notations: z_s is the sprung mass displacement; z_{us} is the unsprung mass displacement; z_r is the pavement defect; K_s is the spring stiffness; K_{us} is the tire stiffness; C_s is the damper damping factor; $C_{us} \approx 0$ is the tire damping factor; finally, u is a control signal.

Following [17], we use the suspension parameters $K_s = 17765$ N/m, $K_{us} = 190125$ N/m, $C_s = 535$ N·s/m, $m_s = 285$ kg, and $m_{us} = 41$ kg. The value $(z_s - z_{us})$ characterizes the suspension deflection, and $\ddot{z}_s$ is the vertical acceleration of the vehicle body.

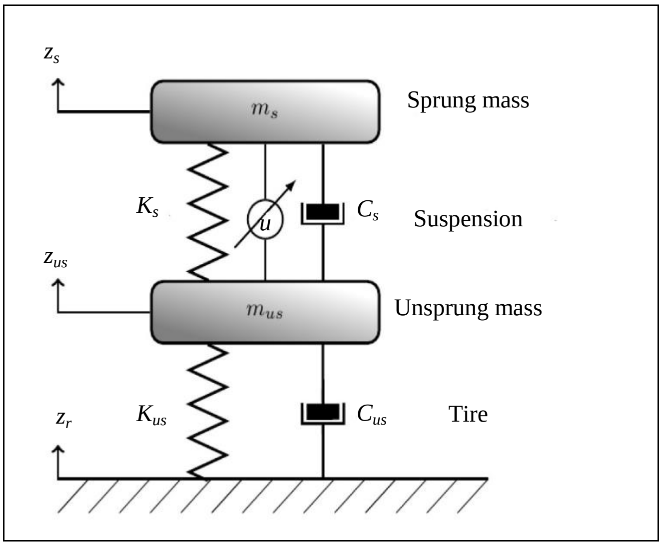

Fig. 1. The linear active quarter-car model.

Ride comfort is characterized by the *root mean square* (RMS) value of the vertical vehicle acceleration. The lower this value is, the higher the comfort level will be. On the other hand, road handling is characterized by the duration of the wheel's contact with the road surface. The greater the RMS value of the suspension deflection is, the lower the road handling level will be.

There is an unavoidable contradiction between ride comfort and road handling since the wheel position approximates the road profile at low frequencies (< 5 rad/s): any decrease in the body travel (vertical position of the sprung mass) at these frequencies will increase the suspension deflection [18]. To resolve this contradiction, this paper considers an adaptive ADRC-based control strategy.

2. ADAPTIVE CONTROL OF ACTIVE DISTURBANCE SUPPRESSION

As stated in [10], both road handling and ride comfort depend on the suspension travel z_s. According to the authors, the suspension travel value should be assigned by prioritizing one of the two aspects. Moreover, a possible way to improve suspension performance is to increase passenger comfort when the relative displacement between the sprung and unsprung masses is far enough from the suspension limits. On the other hand, the control unit must provide safe handling by limiting the suspension travel.

To simplify the idea, consider the control scheme in Fig. 2. Assume that the controller's feedback is given by $(z_s - \alpha z_{us})$, where $\alpha \in [0, 1]$ is the tuning parameter. For $\alpha = 0$, the feedback input is z_s. (In other words, the algorithm aims to minimize the vertical displacement of the sprung mass.) As a consequence, vertical acceleration will be minimized, providing the necessary comfort. When α increases, the suspension travel becomes greater, and the controller gradually gives priority to reducing the suspension travel.

In this paper, we apply ADRC to utilize its adaptive capabilities. In this case, the focus is on an appropriate variation law of the parameter α when changing the suspension deflection.

3. DESCRIPTION OF ADRC

ADRC is an inheritor of the proportional-integral-differential (PID) controller and can be considered a reliable control method: it represents all the unknown dynamics not included in the mathematical model of the controlled system and compensates model uncertainties and exogenous disturbances in real time [19].

As a result, the controlled system behaves like an nth-order integrator $(1/s^n$, where s denotes the Laplace variable and n expresses the system order).

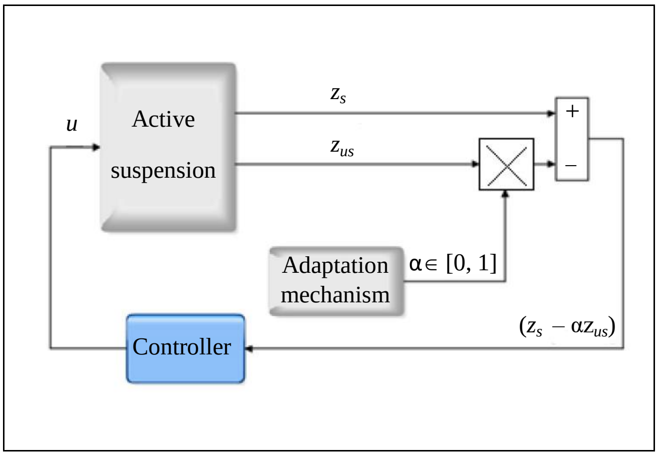

Fig. 2. The control scheme proposed for the handling-comfort trade-off.

Therefore, it is easily controlled by a proportional-differential (PD) controller, even in the case of a nonlinear and time-invariant plant. Figure 3 shows the nonlinear structure of ADRC with four main blocks: the controller (nonlinear state error feedback, NLSEF), the extended state observer (ESO), the tracking differentiator (TD), and the disturbance rejection scheme (DRS).

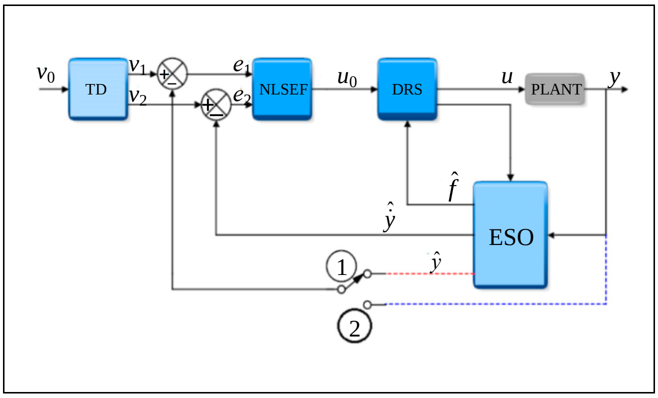

Fig. 3. The diagram of ADRC.

ADRC does not require a precise system model. By assumption, system dynamics can be expressed in the general form

$$\ddot{y} = b_0 u + f, \tag{1}$$

with the following notations: y is the output signal; u is the control input; f is the total disturbances containing the exogenous and endogenous ones; b_0 is the plant's gain.

The reference signal is smoothed by the TD, and the output signals are generated to track the reference signal and its differential. The algorithm is written as

$$\dot{v}_1 = v_2,\ \dot{v}_2 = f_{td}(v_1 - v_0, v_2, r_1) = \\ -r\,\mathrm{sign}\left(v_1 - v_0 + \frac{v_2|v_2|}{2r_1}\right),$$

with the following notations: v_0 is the desired input; v_1 is the tracking signal of the system; v_2 is the differential signal of the system; r_1 is the parameter determining the tracking rate. As proposed in [19], the nonlinear function f_{td} ensures the fastest possible tracking of the reference signal and its derivative considering the acceleration limit r_1. The parameter r_1 depends on the application and is tuned accordingly to speed up or slow down the transients.

A conventional ESO is used to estimate system dynamics. This observer yields the estimates $\hat{y} \approx y$, $\hat{\dot{y}} \approx \dot{y}$, and $\hat{f} \approx f$ (the exogenous disturbances and endogenous dynamic uncertainties). The ESO monitors the performance and forecasts the plant's state in real time. This process was described in the paper [19]:

$$\hat{e} = z_1 - y,\ \dot{z}_1 = z_2 + \alpha_1 \hat{e},$$

$$\dot{z}_2 = z_3 + \alpha_2 |\hat{e}|^{1/2}\,\mathrm{sign}(\hat{e}) + \hat{b}_0 u,$$

$$\dot{z}_3 = \alpha_3 |\hat{e}|^{1/4}\,\mathrm{sign}(\hat{e}),$$

where: y is the system output; z_1 is the tracking signal for y; $\hat{e}$ is the estimated error; z_2 is the differential signal for z_1; z_3 is the tracking signal for the total disturbances; α_1, α_2, and α_3 are the estimation coefficients; u is the control input; $\hat{b}_0$ is the system coefficient (the estimated value of the gain b_0).

The nonlinear state error feedback is a nonlinear control strategy that can improve the accuracy of the control system. As described in [19], it has the form

$$\hat{e}_1 = v_1 - z_1,\ \hat{e}_2 = v_2 - z_2,$$

$$u_0 = \beta_1 f_{nl}(\hat{e}_1, \gamma_1, \eta) + \beta_2 f_{nl}(\hat{e}_2, \gamma_2, \eta), \qquad (2)$$

$$u = \frac{u_0 - z_3}{b_0},$$

with the following notations: $\hat{e}_1$ is the estimated system error; $\hat{e}_2$ is the estimated system error differential; β_1 and β_2 are the gains; the function f_{nl} should provide good control efficiency and high-frequency switching between the modes. Following [19], it can be chosen as

$$f_{nl}(e, \gamma, h) = \begin{cases} \dfrac{e}{\eta^{\gamma-1}}, & |e| \le \eta, \\ |e|^{\gamma}\,\mathrm{sign}(e), & |e| > \eta. \end{cases}$$

Note that the disturbance rejection scheme (DRS) is the last part of equation (2):

$$u = \frac{u_0 - z_3}{b_0},$$

where the estimated disturbance $z_3 = \hat{f}$ is eliminated by subtracting it from the control signal u_0.

Figure 3 shows a switch with two different modes (1 and 2). Thus, the output signal y can be directly passed to the NLSEF controller instead of its estimate $\hat{y}$.

4. AUTOMATIC TUNING OF THE PARAMETER α

We return to the system dynamics (1). Due to the input of the control system (system output) $y = z_s - \alpha z_{us}$, the following fact seems clear: if the closed-loop system is stable, the drift value f will change almost linearly with changing the amplitude of the road disturbances. See Fig. 4, where the values of f are compared with the amplitude of the road disturbances for the closed loop of the sprung mass displacement in the quarter-car model stabilized by ADRC. At the same time, the suspension deflection is inversely proportional to the values of the function f.

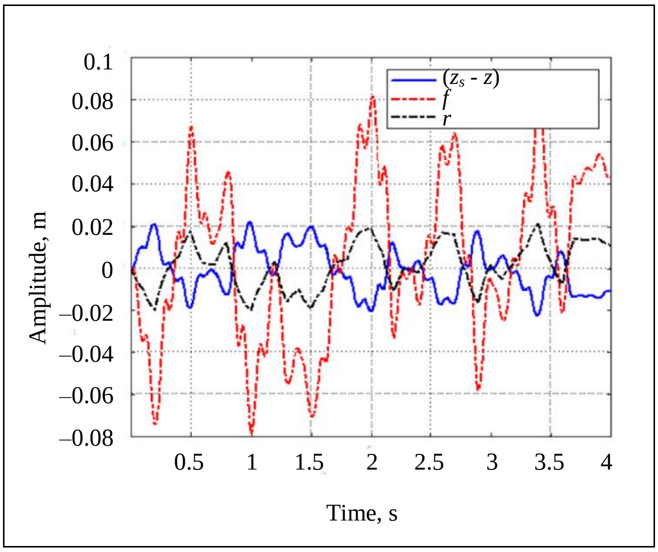

Fig. 4. Values of the function *f* depending on road disturbances.

The parameter α should grow significantly as the suspension deflection increases to balance between the suspension deflection and the passenger comfort.

Therefore, we apply *the MIT rule* with a positive gradient to obtain the variation law of α. In this case, the suspension deflection can be considered a linear function of *f*:

$$z_s - z_{us} = T_{K,w}(f),$$

where $T_{K,w}$ is a *low pass filter* (LPF) with a gain K and a cut-off frequency w. The filter gain and pass frequency are tuning parameters. The performance index α will depend on the absolute value of the suspension deflection, which can be chosen as follows:

$$J(\alpha) = \frac{1}{2}\left(z_s(\alpha) - z_{us}(\alpha)\right)^2.$$

Applying the inversion of the MIT gradient rule to increase the quadratic performance index as the suspension deflection grows, we obtain

$$\frac{\partial J}{\partial\left(z_s(\alpha) - z_{us}(\alpha)\right)} = z_s(\alpha) - z_{us}(\alpha) = T_{K,w}(f),$$

$$\frac{d\alpha}{dt} = \gamma\frac{\partial J}{\partial\alpha} = \gamma\frac{\partial J}{\partial\left(z_s(\alpha) - z_{us}(\alpha)\right)} \times$$

$$\frac{\partial\left(z_s(\alpha) - z_{us}(\alpha)\right)}{\partial\alpha} = \gamma T_{K,w}(f)\frac{\dot{T}_{K,w}(f)}{\dot{\alpha}}$$

$$\Downarrow$$

$$\left(\dot{\alpha}\right)^2 = \gamma T_{K,w}(f)\dot{T}_{K,w}(f) \Rightarrow \dot{\alpha} = \rho\sqrt{T_{K,w}(f)\dot{T}_{K,w}(f)},$$

where $\gamma > 0$ is the tuning parameter, and $\rho = \sqrt{\gamma}$. To simplify the problem, we assume that $\dot{T}_{K,w}(f) = T_{K,w}(\dot{f})$. Hence, the variation rule of the parameter α takes the form

$$\dot{\alpha} = \rho\sqrt{T_{K,w}(f)T_{K,w}(\dot{f})},$$

where ρ is the tuning constant.

Permanent integration of the parameter α will lead to saturation over time, and integration here can be treated as finding the envelope. This is true because the values of α should decrease if the suspension deflection grows over time and increase otherwise.

In applications, this can easily be achieved by adding a simple envelope calculation scheme or equivalent mathematical equations to filter the estimated value of α.

Figure 5 shows the complete control scheme of the system. The Kalman filter extracts the displacements z_s and z_{us} separately using the sensor outputs (a vertical acceleration sensor for the sprung mass, a vertical acceleration sensor for the unsprung mass, and a potentiometer for the suspension deflection). Let the system be equipped with two types of sensors: (1) two acceleration sensors to measure the acceleration of the sprung and unsprung mass, respectively, and (2) a potentiometer to measure the suspension deflection.

The linear Kalman filter is based on the equations

$$\begin{aligned}\dot{x}_1 &= x_2,\\ \dot{x}_2 &= m_1,\\ \dot{x}_3 &= x_4,\\ \dot{x}_4 &= m_2,\end{aligned} \quad y_e = \begin{pmatrix} x_1 \\ x_3 \\ x_1 - x_3 \end{pmatrix}, \quad y_m = \begin{pmatrix} \iint m_1 \\ \iint m_2 \\ m_3 \end{pmatrix}, \tag{3}$$

$$A = \begin{pmatrix} 0 & 1 & 0 & 0 \\ 0 & 0 & 0 & 0 \\ 0 & 0 & 0 & 1 \\ 0 & 0 & 0 & 0 \end{pmatrix}, B = \begin{pmatrix} 0 \\ m_1 \\ 0 \\ m_2 \end{pmatrix}, C = \begin{pmatrix} 1 & 0 & 0 & 0 \\ 0 & 0 & 1 & 0 \\ 1 & 0 & -1 & 0 \end{pmatrix}, \tag{4}$$

with the following notations: *A*, *B*, and *C* are the state, control, and output matrices, respectively; m_1 and m_2 are the measured accelerations of the sprung and unsprung mass, respectively; m_3 is the measured suspension deflection; y_e and y_m are the estimation and measurement vectors, respectively; finally, $\begin{pmatrix} x_1 & x_2 & x_3 & x_4 \end{pmatrix}^{\mathrm{T}} = \begin{pmatrix} z_s & \dot{z}_s & z_{us} & \dot{z}_{us} \end{pmatrix}^{\mathrm{T}}$.

Formulas (3) and (4) are the state-space representation of the two second-order integrators. These integrators yield the positions z_s and z_{us} from the measured accelerations $\ddot{z}_s$ and $\ddot{z}_{us}$. The measured suspension deflection $(z_s - z_{us})$ is used to correct the estimated positions at each time instant, being added to the measurement vector y_m. Without including the measured suspension deflection in the measurement vector, the positions z_s and z_{us} will have constant deflection deviations from the real values.

The covariance matrices for the process and observation noises can be chosen empirically. The initial value of the estimation covariance is chosen large enough, and the initial state estimate is zero.

The values of the parameter $\dot{\alpha}$ are passed to the envelope detector and are limited to the range [0, 1]; see Fig. 5. Here, v_0 is the desired input (zero in the presented approach). Therefore, the TD is irrelevant in this figure: it appears only to preserve the overall ADRC form.

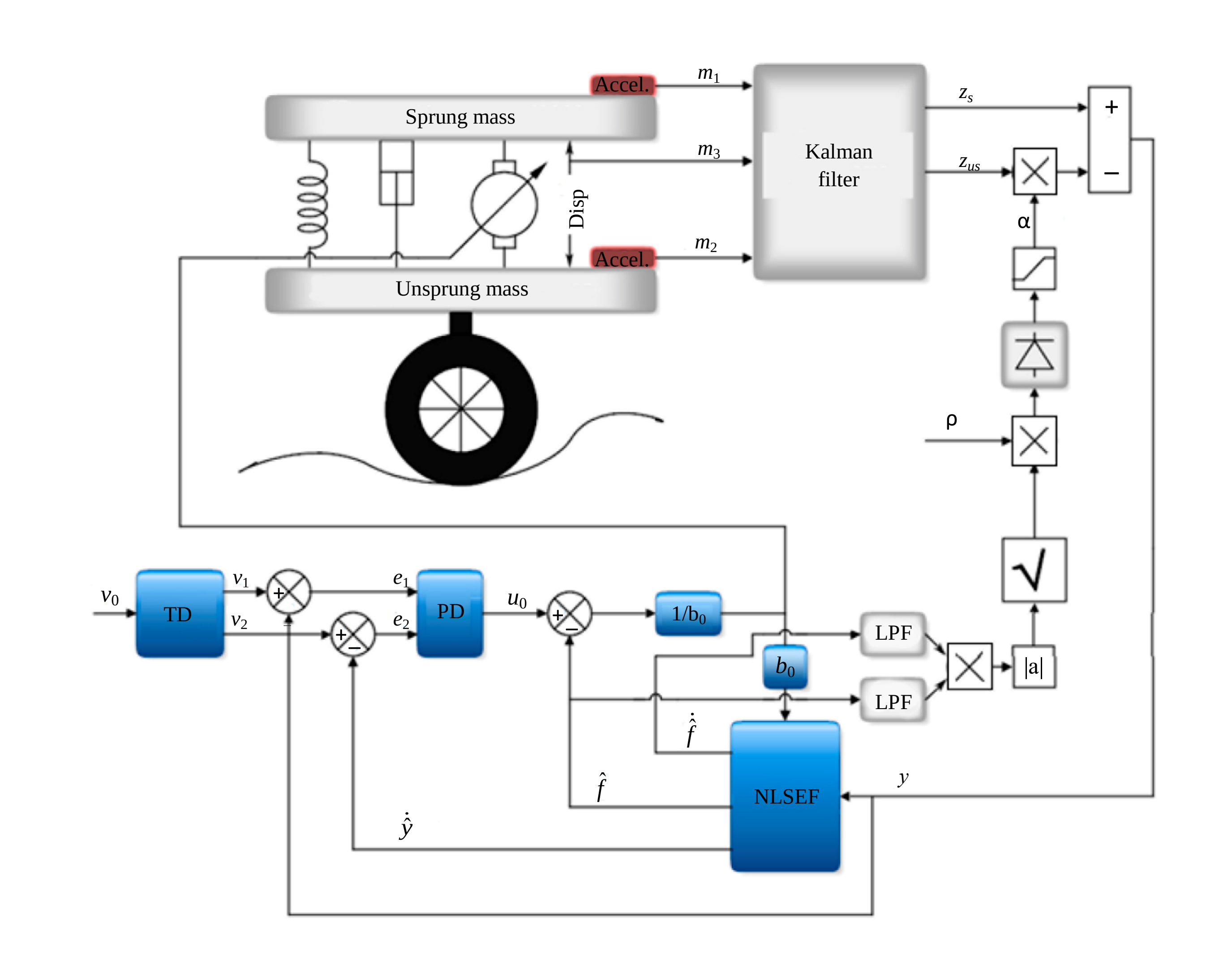

Fig. 5. Adaptive control system (complete diagram).

To demonstrate the effectiveness of this adaptive control law, we estimate the system performance in two cases. In the first case, the road disturbances are random (the ISO-8608 standard), and the system focuses on passenger comfort. In the second case, a sudden shock is treated as a roadblock: when it occurs, the driver is expected to focus on road handling (not to lose control of the vehicle).

To make the simulation more realistic, we choose a hydraulic active system of the quarter-car type with the nonlinear hydraulic actuator model.

5. SIMULATION

This section describes the hydraulic active system of the quarter-car type, the road disturbances, and the simulation results of the adaptive controller.

5.1 Hydraulic active system of the quarter-car type

The active suspension system uses a hydraulic actuator to reduce the external power required to achieve the desired performance. This system exerts an independent impact on the suspension to improve ride quality. The vehicle's active suspension system is presented in Fig. 6.

The hydraulic actuator consists of a spool (servo) valve and a hydraulic cylinder. Figure 6 has the following notations: P_s and P_r are the pressure of the hydraulic fluid entering and leaving the spool valve, respectively; x_{sp} is the position of the spool valve; P_u and P_l are the oil pressure in the upper and lower cylinder chambers, respectively. When the spool valve moves upwards (positive value), the upper chamber of the cylinder is connected to the supply line, and its

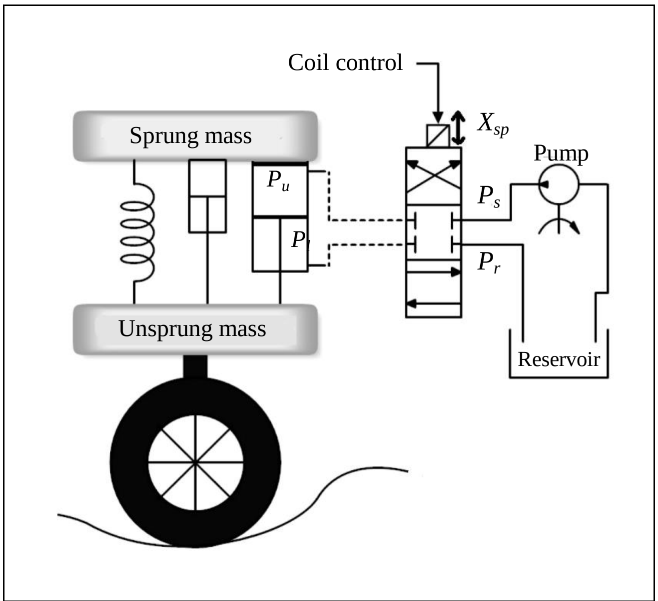

Fig. 6. Active hydraulic suspension system.

pressure increases. Meanwhile, the lower chamber is connected to the return valve, and its pressure decreases. This pressure difference expands the hydraulic cylinder.

For a mechanical movement of the valve spool, an electric current is applied to the coil connected to the servo valve. The powered actuator drives the spool to the desired position.

The actuator is described by the equation

$$v_c = L_c \frac{di_{sv}}{dt} + R_c i_{sv} \Rightarrow \frac{I_{sv}}{V_c} = \frac{1}{L_c s + R_c},$$

with the following notations: R_c and L_c are the coil resistance and inductance, respectively; v_c and i_{sv} are the motor rotor voltage and current, respectively. In the expressions below, the transition from lowercase to uppercase symbols means the variables in the Laplace space.

Let the spool valve displacement x_{sp} be related to the servo valve current i_{sp} through the linear transfer function

$$\frac{X_{sp}}{I_{sv}} = \frac{w_n^2}{s^2 + 2\xi w_n s + w_n^2}, \tag{5}$$

where ξ is the damping coefficient, and w_n is the natural frequency of the servo valve. By a common assumption, the dynamics (5) are very fast, and we write

$$\frac{X_{sp}}{V_c} \approx \frac{K_v}{\tau s + 1},$$

where τ is the time constant of the servo valve, and K_v is the gain constant.

We introduce several assumptions:

– The valve area is linearly related to the spool displacement.

– The piston area is much larger than the bore.

– The fluid is incompressible.

– The inertia of the piston is negligible.

– The pressure changes in the two chambers are approximately equal, i.e.,

$$\Delta P_u \approx -\Delta P_l = \Delta P.$$

Then the impact is defined as

$$F_a = A_p \Delta P,$$

where A_p is the average piston area, and ΔP is the pressure difference in the valve pipelines. Following [20], this difference can be calculated by

$$\frac{V_t}{4\beta_e} \Delta \dot{P} = Q - C_{tp} \Delta P - A_p (\dot{z}_s - \dot{z}_{us}),$$

with the following notations: V_t is the total cylinder volume; β_e is the effective volume modulus; Q is the hydraulic load flow; C_{tp} is *the total piston leakage rate*. The flow equation with the controlled servo valve load has the form

$$Q = \text{sign}[P_s - \text{sign}(x_{sp})\Delta P] C_d w_g \times$$
$$x_{sp} \sqrt{\frac{1}{\rho_1}(P_s - \text{sign}(x_{sp})\Delta P)}, \tag{6}$$

where C_d is the *discharge coefficient*, w_g is the spool valve area gradient, and ρ_1 is the hydraulic fluid density. With the variables

$$\alpha_1 = 4\beta_e / V_t,\ \beta = \alpha_1 C_{tp},\ \gamma = \alpha_1 C_d w_g \sqrt{1/\rho_1},$$

the system dynamics can be represented in the state space, as in equation (6):

$$X_1 = z_s,\ X_2 = \dot{z}_s,\ X_3 = z_{us},\ X_4 = \dot{z}_{us},$$
$$X_5 = \Delta P,\ X_6 = x_{sp},\ \dot{X}_1 = X_2,$$
$$\dot{X}_2 = -\frac{1}{M_s}\big(K_s(X_1 - X_3) + C_s(X_2 - X_4) - A_p X_5\big),$$
$$\dot{X}_3 = X_4,$$
$$\dot{X}_4 = \frac{1}{M_{us}}\big(K_s(X_1 - X_3) + C_s(X_2 - X_4) -$$
$$K_{us}(X_3 - z_r) - C_{us}(X_4 - \dot{z}_r) - A_p X_5\big),$$

$$\dot{X}_5 = -\beta X_5 - \alpha_1 A_p (X_2 - X_4 + \gamma X_6 \nu),$$

$$\dot{X}_6 = \frac{1}{\tau}(-X_6 + K_v u),\ u = V_c,$$

$$\nu = \mathrm{sign}[P_s - \mathrm{sign}(X_6)X_5]\sqrt{P_s - \mathrm{sign}(X_6)X_5}.$$

We chose the following parameters to simulate the nonlinear model of the electrohydraulic actuator system:

$$\alpha = 4.515\times10^{13}\ \mathrm{N/m^5},\ \beta = 1\ s^{-1},$$

$$\gamma = 1.545\times10^{9}\ \mathrm{N/m^{5/2}kg^{1/2}},$$

$$\tau = \frac{1}{30}\mathrm{s},\ K_v = 4\times10^{-3},\ A_p = 3.35\times10^{-4}\ \mathrm{m^2}.$$

The source and external pressures were set to P_s = 10 bar and P_r = 1 bar, respectively.

5.2 Models of road disturbances

Following the ISO-8608 standard [9], a random filtered disturbance in the time domain was used as road disturbances to test the comfort level. The corresponding differential equation has the form

$$\dot{q}(t) = -2\pi f_0 q(t) + 2\pi n_0 \sqrt{G_q(n_0)v}\, w_d(t),$$

with the following notations: $q(t)$ is the random input signal; f_0 is a filter with a lower cutoff frequency; $G_q(n_0)$ is the road roughness coefficient; $w_d(t)$ is the Gaussian white noise. The vehicle speed was set to $v = 54$ km/h. A C class road was considered: $G_q(n_0) = 512\times10^{-6}$ and $n_0 = 0.1$.

For the handling test, the road shock was described by

$$w_d(t) = \begin{cases} 0.5h(1-\cos(w_b t)), & t_1 \le t \le t_2, \\ 0, & \text{otherwise}, \end{cases}$$

where: h = 0.1 m and w_b are the height and frequency of shocks, respectively; t_1 and t_2 are the lower and upper time limits of the function. The impact frequency is given by $w_b = 2\pi/(t_2 - t_1)$.

5.3 Simulation results

The simulation results are divided into three parts. The first part focuses on ride comfort when the road disturbances are a random signal. The second part concerns vehicle handling when the road disturbances are several consecutive shocks with a given frequency. Finally, the third part considers the two tasks together when the road disturbances of the above types are mixed.

The values of $\dot{\alpha}$ are always positive. Hence, it suffices adding a Butterworth low-pass filter to get the signal envelope. The setting constant for the parameter ρ was set to 200. The low-pass filter was given by $T_{K,w} = 0.1/(0.1s+1)$. The ADRC parameters were assigned as follows:

$$w = 0.5\ \mathrm{rad/s},\ \alpha_1 = 30w,\ \alpha_2 = 15w^2,$$

$$\alpha_3 = 85w^3,\ b_0 = 0.15,\ K_p = w^2,\ K_d = 2w.$$

Figure 7 shows the closed loop response when the road disturbances are random. Clearly, the parameter α has a small value throughout the process: the displacement between the sprung and unsprung masses is still far from its limits. However, the engineer can introduce an additional condition: set α to zero if its value is below some threshold. In this case, the control system will concentrate on ride comfort.

Figure 8 demonstrates the closed loop response when the road disturbances are a sequence of sudden shocks.

Clearly, the parameter α keeps zero values in the absence of exogenous disturbances. Meanwhile, its value gradually grows as the disturbance amplitude increases. Also, the value of α slowly decreases after the shock is over. This situation corresponds to the vehicle's real response to disturbances: the wheels need contact with the road for a short time after the impact is over to ensure greater safety.

For adaptivity tests, we applied this control method to the hydraulic suspension system under the following conditions: a 54 km/h vehicle moving on a C class road (ISO-8608) suddenly encounters several 0.1 m obstacles (in height) in front of it.

Figure 9 shows the closed loop response to these road disturbances. Clearly, the system focuses on ride comfort in the first stage, when the disturbance amplitude is relatively low; it switches to vehicle handling when riding into road bumps. After the high-amplitude disturbances caused by the bumps disappear, the system returns to ride comfort. Note that the proposed control law demonstrates a high degree of flexibility for the disturbances affecting the vehicle. This yields a trade-off between ride comfort and handling using an easily adjusted algorithm requiring no precise knowledge of the system dynamics.

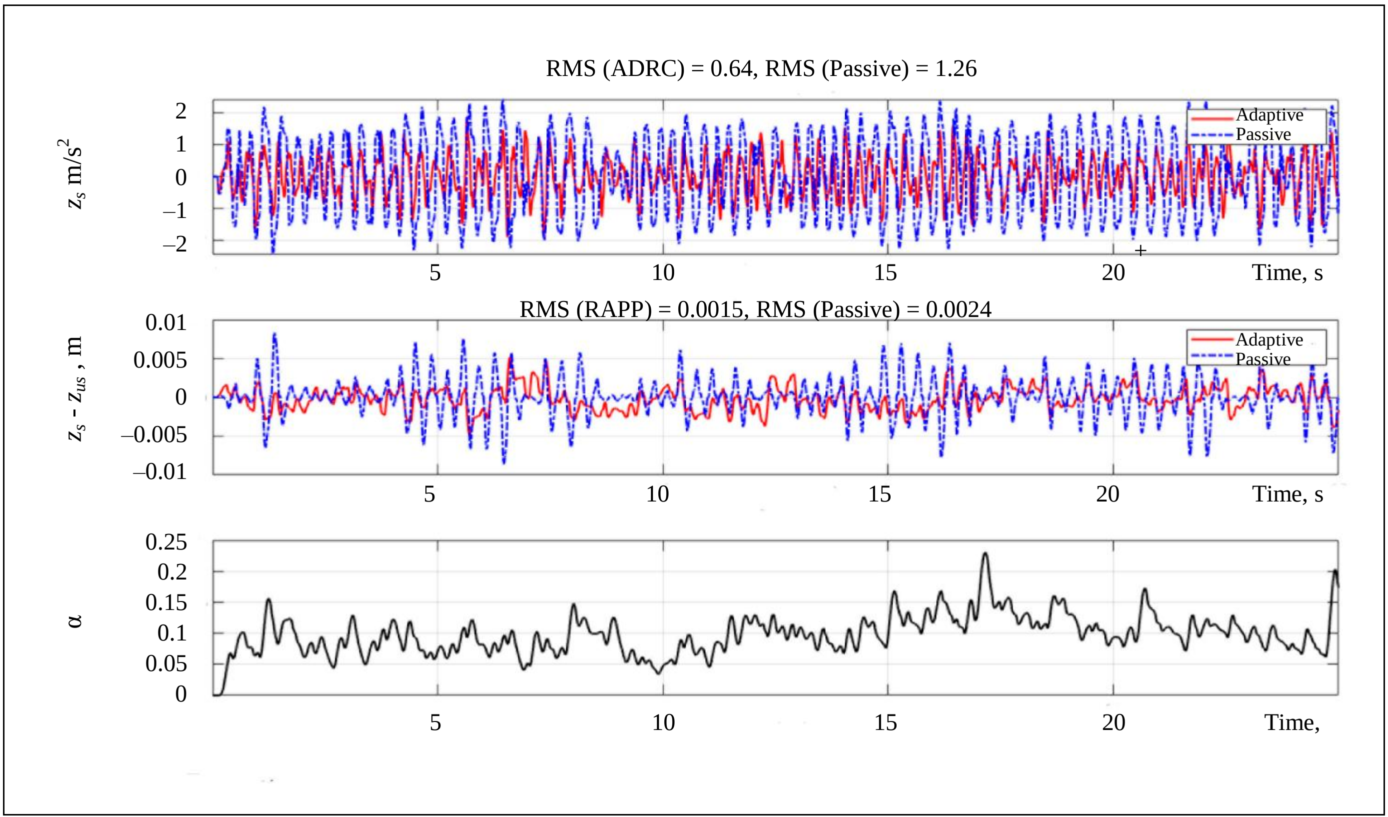

Fig. 7. Simulation results in the case of random road disturbances. The blue lines correspond to the passive system, and the red lines to the adaptive ADRC algorithm.

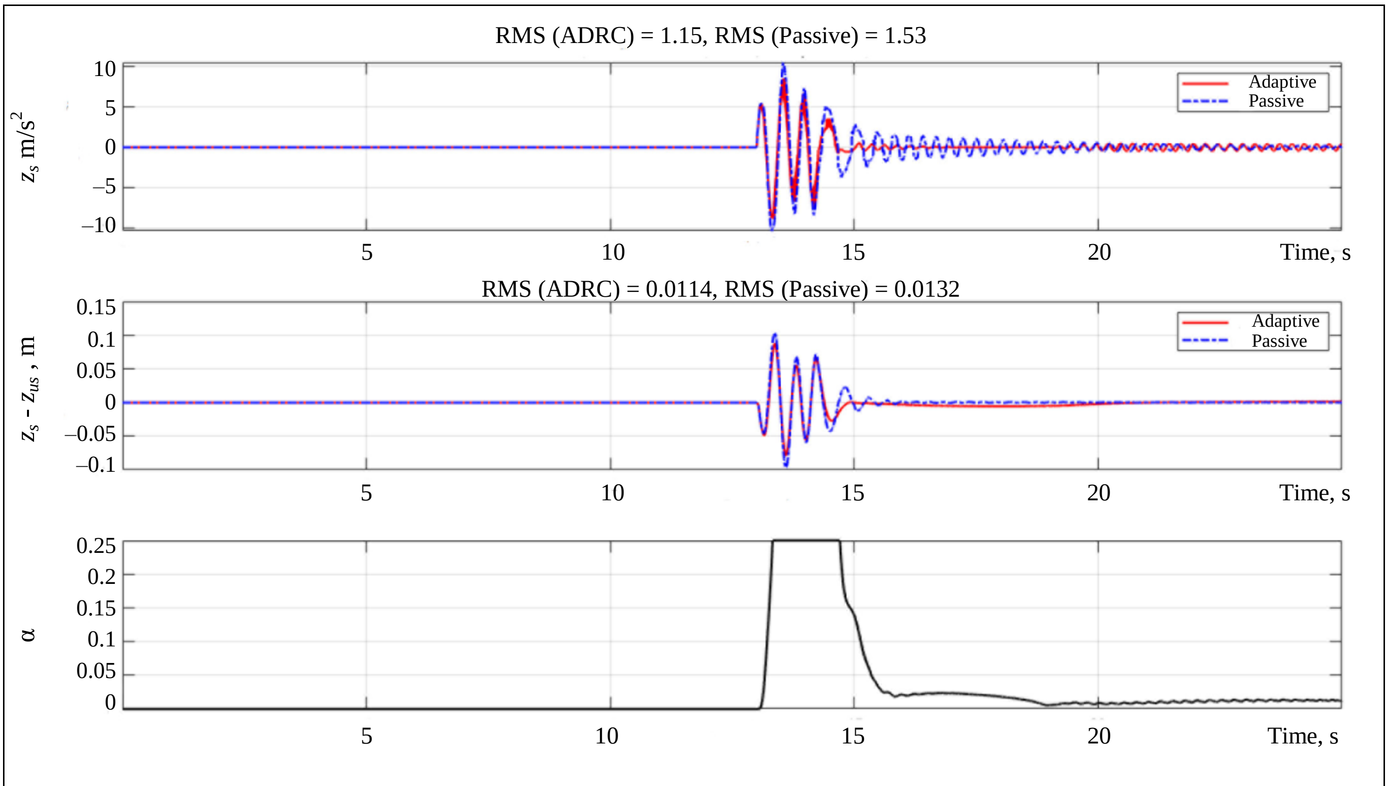

Fig. 8. Simulation results in the case of suddenly riding into road bumps. The blue lines correspond to the passive system, and the red lines correspond to the adaptive ADRC algorithm.

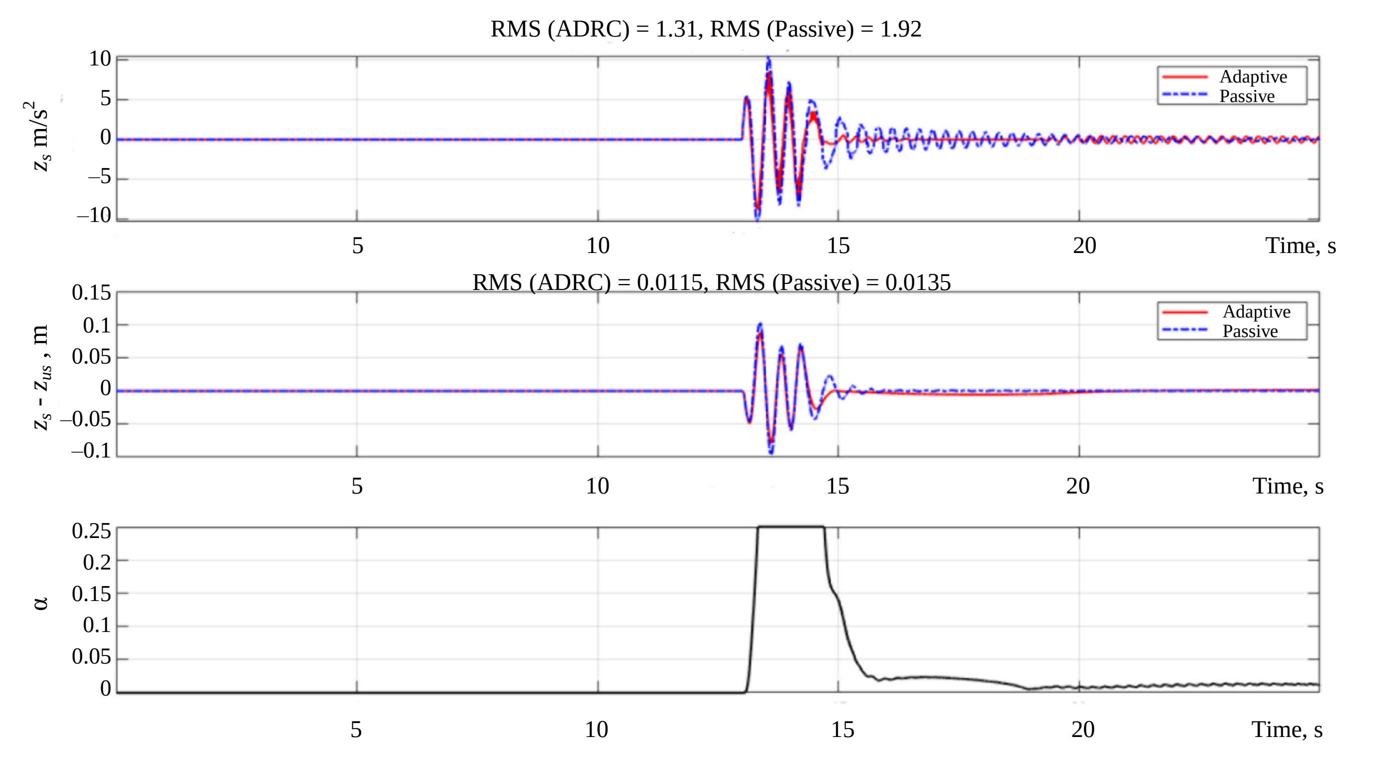

Fig. 9. Closed loop response of the nonlinear quarter-car system to hybrid road disturbances. The first line corresponds to the acceleration of the suspension mass, the second line corresponds to the suspension deflection, and the third line corresponds to the parameter α.

CONCLUSIONS AND FURTHER RESEARCH

This paper has presented a simple approach to managing the trade-off between the vertical acceleration of the vehicle chassis and its position relative to the road surface. Due to the increasing relevance of auto-driving, an auto-tuning ADRC mechanism has been proposed. The basic idea is to use the filtered values of the total disturbances estimated by ADRC to switch the system's operating mode between ride comfort and road handling. This is achieved by embedding the filtered value of the estimated disturbances into the control loop (multiplying this value by the unsprung mass displacement and subtracting it from the sprung mass displacement). The closed loop system has been tested under the following conditions: an average speed vehicle moving on a low-quality road suddenly encounters several obstacles of relatively high height in front of it.

The simulation results have shown the algorithm's ability to adapt and automatically shift focus between ride comfort and road handling. Moreover, this algorithm can be easily tuned for the nonlinear model.

As promising areas of further research, we mention the influence of Kalman filter settings and the change in the road disturbance model on the system performance. In addition, the effect of this controller on the entire vehicle can be studied when maneuvering, turning, and following a given trajectory.

REFERENCES

1. Goodarzi, A. and Khajepour, A., *Vehicle Suspension System Technology and Design*, Kentfield, CA, 2017.
2. Pinkaew, T. and Fujino, Y., Effectiveness of Semi-active Tuned Mass Dampers under Harmonic Excitation, *Engineering Structures*, 2001, vol. 23, no. 7, pp. 850–856.
3. Chaves, M., Maia, J., and Esteves, J., Analysis of an Electromagnetic Automobile Suspension System, *International Conference on Electrical Machines*, Vilamoura, Portugal, 2008.
4. Mihai, I. and Andronic, F., Behavior of a Semi-active Suspension System versus a Passive Suspension System on an Uneven Road Surface, *Mechanics*, 2014, vol. 20, no. 1, pp. 64–69.
5. Zhileykin, M.M., Kotiev, G.O., and Nagatsev, M.V., Synthesis of the Adaptive Continuous System for the Multi-axle Wheeled Vehicle Body Oscillation Damping, *IOP Conference Series: Materials Science and Engineering*, 2018, vol. 315, no. 1.
6. Ovsyannikov, S., Kalinin, E., and Koliesnik, I., Oscillation Process of Multi-support Machines When Driving over Irregularities, in *Energy Management of Municipal Transportation Facilities and Transportation*, Springer, Cham, 2018.
7. Yao, G.Z., Yap, F.F., Chen, G., et al., MR Damper and Its Application for Semi-active Control of Vehicle Suspension System, *Mechatronics*, 2002, vol. 12, no. 7, pp. 963–973.

8. Lajqi, S. and Pehan, S., Designs and Optimizations of Active and Semi-active Non-linear Suspension Systems for a Terrain Vehicle, *Strojniški Vestnik-Journal of Mechanical Engineering*, 2012, vol. 58, no. 12, pp. 732–743.
9. Zhou, Q., Research and Simulation on New Active Suspension Control System, *Master's Thesis*, Lehigh University, 2013.
10. Maizza, G. and Franz, D., *Simulink Control Model of an Active Pneumatic Suspension System in Passenger Cars*, Politecnico di Torino, 2019.
11. Ryu, S., Park, Y., and Suh, M., Ride Quality Analysis of a Tracked Vehicle Suspension with a Preview Control, *Journal of Terramechanics*, 2011, vol. 48, no. 6, pp. 409–417.
12. Tan, B., Wu, Y., Zhang, N., et al., Improvement of Ride Quality for Patient Lying in Ambulance with a New Hydro-Pneumatic Suspension, *Advances in Mechanical Engineering*, 2019, vol. 11, no. 4, pp. 1–20.
13. Abe, M., *Vehicle Handling Dynamics: Theory and Application*, Oxford: Butterworth-Heinemann, 2015.
14. Savsani, V., Patel, V.K., Gadhvi, B., and Tawhid, M., Pareto Optimization of a Half Car Passive Suspension Model Using a Novel Multiobjective Heat Transfer Search Algorithm, *Modelling and Simulation in Engineering*, 2017, vol. 2017, art. ID 2034907.
15. Els, P.S., Theron, N., Uys, P.E., and Thoresson, M., The Ride Comfort vs. Handling Compromise for Off-road Vehicles, *Journal of Terramechanics*, 2007, vol. 44, no. 4, pp. 303–317.
16. Singh, N., Chhabra, H., and Bhangal, K., Robust Control of Vehicle Active Suspension System, *International Journal of Control and Automation*, 2016, vol. 9, no. 4, pp. 149–160.
17. Hasbullah, F., Faris, W., Darsivan, J., and Abdelrahman, M., Ride Comfort Performance of a Vehicle Using Active Suspension System with Active Disturbance Rejection Control, *International Journal of Vehicle Noise and Vibration*, 2015, vol. 11, no. 1, pp. 78–101.
18. de Jesús Lozoya-Santos, J., Tudón-Martínez, J., Morales-Menéndez, R., and Ramírez-Mendoza, R., Comparison of On-off Control Strategies for a Semi-active Automotive Suspension Using HiL, *IEEE Latin America Transactions*, 2012, vol. 10, no. 5, pp. 2045–2052.
19. Han, J., From PID to Active Disturbance Rejection Control, *IEEE Transactions on Industrial Electronics*, 2009, vol. 56, no. 3, pp. 900–906.
20. Pedro, J.O., Dangor, O., Dahunsi, O.A., and Ali, M., CRS and PS-Optimised PID Controller for Nonlinear, Electrohydraulic Suspension Systems, The 9th Asian Control Conference (ASCC), Istanbul, 2013.

This paper was recommended for publication by S.A. Krasnova, a member of the Editorial Board.

Received October 15, 2021, and revised February 15, 2022. Accepted February 28, 2022.

Author information

Alhelou, Muhammed. Postgraduate, Bauman Moscow State Technical University, Moscow, Russia,
✉ alkhelum@student.bmstu.ru

Wassouf, Yazan. Postgraduate, Bauman Moscow State Technical University, Moscow, Russia, ✉ thelegend990@gmail.com

Serebrenny, Vladimir Valer'evich. Cand. Sci. (Eng.), Bauman Moscow State Technical University, Moscow, Russia,
✉ vsereb@bmstu.ru

Gavrilov, Alexander Igorevich. Cand. Sci. (Eng.), Bauman Moscow State Technical University, Moscow, Russia,
✉ alexgavrilov@mail.ru

Lobusov Evgenii Sergeevich. Cand. Sci. (Eng.), Bauman Moscow State Technical University, Moscow, Russia,
✉ evgeny.lobusov@yandex.ru

Cite this paper

Alhelou, M., Wassouf, Y., Serebrenny, V.V., Gavrilov, A.I., and Lobusov, E.S., The Handling-Comfort Trade-Off in a Quarter-Car System: Automatic Adaptive Management via Active Disturbance Rejection Control. *Control Sciences* **2,** 29–39 (2022). http://doi.org/10.25728/cs.2022.2.4

Translated into English by *Alexander Yu. Mazurov*,
Cand. Sci. (Phys.-Math.),
Trapeznikov Institute of Control Sciences,
Russian Academy of Sciences, Moscow, Russia
✉ alexander.mazurov08@gmail.com